arXiv:hep-ph/0112145v1 11 Dec 2001

$\Lambda_b \to \Lambda J/\psi$ decay in perturbative QCD

Chung-Hsien Chou[*], Hsien-Hung Shih[†], Shih-Chang Lee[‡], and Hsiang-nan Li[§]
Institute of Physics, Academia Sinica, Taipei, Taiwan 115, Republic of China

(February 1, 2008)
PACS numbers: 12.38.Bx, 12.38.Cy, 13.30.Ce, 12.39.Fe, 11.30.Rd

We calculate the amplitudes involved in the heavy baryon nonleptonic decay $\Lambda_b \to \Lambda J/\psi$ using perturbative QCD factorization theorem, which are expressed as convolutions of hard b quark decay amplitudes with the Λ_b baryon, Λ baryon and J/ψ meson distribution amplitudes. It is found that nonfactorizable contributions dominate over factorizable ones. Because of soft cancellation in pairs of nonfactorizable diagrams, the $\Lambda_b \to \Lambda J/\psi$ decay is characterized by a large scale, such that perturbative QCD is applicable. Employing the distribution amplitudes determined in our previous works and from QCD sum rules, we derive the branching ratio $B(\Lambda_b \to \Lambda J/\psi) = (1.7 \sim 5.3) \times 10^{-4}$ in agreement with data. We predict an asymmetry parameter $\alpha = -0.17 \sim -0.14$ associated with the anisotropic angular distribution of the Λ baryons produced in polarized Λ_b baryon decays.

I. INTRODUCTION

Recently, we have developed perturbative QCD (PQCD) factorization theorem for the semileptonic heavy baryon decays $\Lambda_b \to pl\bar{\nu}$ [1] and $\Lambda_b \to \Lambda_c l\bar{\nu}$ [2,3]. This theorem states that nonperturbative dynamics involved in a high-energy QCD process can be factorized into hadron distribution amplitudes, and the remaining piece is calculable in perturbation theory. A distribution amplitude, though not calculable, is universal. Once a distribution amplitude is determined from experimental data of some processes, it can be employed to make predictions for other processes involving the same hadron. According to this theorem, the form factors involved in the decay $\Lambda_b \to \Lambda_c l\bar{\nu}$ have been expressed as the convolutions of hard b quark decay amplitudes with the universal Λ_b and Λ_c baryon distribution amplitudes. It has been found that perturbative contributions to the $\Lambda_b \to \Lambda_c$ decays become more important at the maximal recoil of the Λ_c baryon with the velocity transfer about 1.4. This observation indicates that PQCD is an appropriate tool for analyses of two-body nonleptonic Λ_b baryon decays.

An essential feature of PQCD [4–8] is that it goes beyond the conventional approach to exclusive nonleptonic heavy hadron decays based on the factorization approximation (FA) [9]. Both factorizable and nonfactorizable contributions from various topologies (emission and annihilation) can be evaluated systematically in PQCD. Though nonfactorizable contributions are usually negligible, they become dominant in the modes $B \to J/\psi K^{(*)}$ [10], whose factorizable contributions arise from internal W-emission with the small Wilson coefficient a_2 defined below. This is the reason it is difficult to accommodate the data of the ratios $R = B(B \to J/\psi K^*)/B(B \to J/\psi K)$ and $R_L = B(B \to J/\psi K^*_L)/B(B \to J/\psi K^*)$ simultaneously in FA. However, these data can be explained in the PQCD formalism [7].

In this paper we shall extend PQCD factorization theorem to the more complicated baryon decay $\Lambda_b \to \Lambda J/\psi$, and show that nonfactorizable contributions also play an essential role. A simple investigation indicates that each diagram for the $\Lambda_b \to \Lambda J/\psi$ decay is characterized by the scale $\bar{\Lambda}$, where $\bar{\Lambda} = M_{\Lambda_b} - m_b$ is the mass difference between the Λ_b baryon and the b quark. Factorizable contributions, having this low typical scale, are suppressed by the Wilson coefficient a_2. The dominant nonfactorizable contributions, due to soft cancellation between a pair of diagrams, are characterized by the higher scale $\sqrt{\bar{\Lambda} M_{\Lambda_b}[1 - (M_{J/\psi}/M_{\Lambda_b})^2]}$, with $M_{J/\psi}$ being the J/ψ meson mass. Therefore, the $\Lambda_b \to \Lambda J/\psi$ decay is a special heavy-to-heavy mode, to which PQCD is applicable.

The Λ_b baryon distribution amplitude has been chosen to satisfy the experimental upper bound of the $\Lambda_b \to \Lambda_c l\bar{\nu}$ branching ratio and the requirement of heavy quark symmetry [2]. The J/ψ meson distribution amplitudes have been determined from the experimental data of the $B \to J/\psi K^{(*)}$ decays [7]. The Λ baryon distribution amplitudes have been derived from QCD sum rules [11,12]. We shall employ these distribution amplitudes, because of their universality, to predict the branching ratio $B(\Lambda_b \to \Lambda J/\psi)$. We also consider another interesting quantity, the

---

[*] chouch@phys.sinica.edu.tw
[†] hhshih@phys.sinica.edu.tw
[‡] phsclee@ccvax.sinica.edu.tw
[§] hnli@phys.sinica.edu.tw

asymmetry parameter α defined in Sec. V, which is related to the anisotropic angular distribution of the Λ baryons produced in polarized Λ_b baryon decays.

The $\Lambda_b \to \Lambda J/\psi$ decay has been discussed in the quark model based on FA [13]. Our predictions

$$\begin{aligned} &B(\Lambda_b \to \Lambda J/\psi) = (1.7 \sim 5.3) \times 10^{-4} \;, \\ &\alpha = -0.17 \sim -0.14 \;, \end{aligned} \tag{1}$$

are consistent with those from FA. However, the theoretical bases of the two approaches are quite different: nonfactorizable contributions are neglected, and the Wilson coefficient a_2 is treated as a free parameter in FA. We emphasize that there is no free parameter in the PQCD calculation. The comparison of our predictions with data will provide a justification of the PQCD formalism for heavy baryon decays.

In Sec. II we briefly review factorization theorem for exclusive nonleptonic heavy hadron decays. The hadron distribution amplitudes and the associated Sudakov factors are defined in Sec. III. The factorization formulas for the $\Lambda_b \to \Lambda J/\psi$ decay amplitudes are presented in Sec. IV. Numerical results are discussed in Sec. V. Section VI is the conclusion. To deliver our ideas clearly, we shall leave all technical calculations and complicated expressions to the Appendices. Appendix A contains the useful integrals employed in this work and the measures of phase-space integrations for different diagrams. The hard amplitudes are summarized in Appendices B and C.

II. FACTORIZATION THEOREM

We briefly review PQCD factorization theorem for exclusive nonleptonic heavy hadron decays [6], and discuss its application to the $\Lambda_b \to \Lambda J/\psi$ mode. The effective Hamiltonian responsible for this mode is expressed as

$$\mathcal{H}^{\rm eff} = \frac{G_F}{\sqrt{2}} V_{cb} V_{cs}^* [\, C_1(\mu) O_1(\mu) + C_2(\mu) O_2(\mu) \,] \;, \tag{2}$$

where G_F is the Fermi coupling constant, V's the Cabibbo-Kobayashi-Maskawa matrix elements, $C_{1,2}(\mu)$ the Wilson coefficients, and μ an arbitrary renormalization scale. The four-fermion operators $O_{1,2}$ are written as

$$O_1 = (\bar{c}b)(\bar{s}c) \;, \quad O_2 = (\bar{s}b)(\bar{c}c) \;, \tag{3}$$

with $(\bar{q}_1 q_2) = \bar{q}_1 \gamma_\mu (1-\gamma_5) q_2$ being the $V-A$ current.

We shall have a careful look at the derivation of the above effective Hamiltonian starting with eight-quark amplitudes (three quarks from the Λ_b baryon, three quarks from the Λ baryon and two quarks from the J/ψ meson). The lowest-order diagrams contain one W boson for the weak decay of the b quark and two hard gluons attaching the spectator quarks. Nonleptonic Λ_b baryon decays involve three scales: the W boson mass M_W, at which the matching conditions of the effective Hamiltonian are defined, the hard scale t related to M_{Λ_b}, which reflects specific dynamics of different modes, and the factorization scale of $O(\bar{\Lambda})$ [6]. The factorization scale is introduced to separate perturbative contributions from nonperturbative contributions absorbed into hadron distribution amplitudes $\phi(x,b)$, x being a momentum fraction carried by one of the valence quarks. In the PQCD formalism the factorization scale is chosen as $1/b$, b being the transverse extent of a hadron.

Radiative corrections generate various types of large logarithms, such as $\alpha_s \ln(M_W/t)$ and $\alpha_s \ln(tb)$, which should be summed by renormalization-group (RG) methods to give evolution factors. The Wilson coefficients $C(t)$ from the summation of the first type of logarithms correspond to the evolution from M_W to t. The second type of logarithms is summed to give the evolution $g(t,b)$ from t to $1/b$, which is governed by an anomalous dimension different from that of $C(t)$. The difference arises from the loop corrections to the eight-quark amplitudes for $g(t,b)$, and those to the four-quark amplitudes associated with the W boson exchange for $C(t)$ [14]. There also exist double logarithms $\alpha_s \ln^2(Pb)$, P being the dominant light-cone component of hadron momentum, which appear in radiative corrections to hadron wave functions. These logarithms, from the overlap of collinear and soft divergences, are treated by the resummation technique [15,16]. The result is a Sudakov exponential $\exp[-s(P,b)]$, which decreases fast with b and vanishes at $b = 1/\Lambda_{\rm QCD}$, $\Lambda_{\rm QCD}$ being the QCD scale. Since the Sudakov factor supresses long-distance contributions from the large b region [17,18], the hard scale t, always larger than the factorization scale $1/b$, does not go down to $\bar{\Lambda}$.

After summing logarithmic corrections, the hard amplitude $H(t)$ can be calculated perturbatively by means of Feynman diagrams with on-shell external quarks. The on-shellness in the present leading-power analysis means that the virtualities of the external quarks are at most of $O(\bar{\Lambda}/m_b)$. The $\Lambda_b \to \Lambda J/\psi$ hard amplitude contains both factorizable and nonfactorizable internal W-emission contributions from the lowest-order diagrams in Fig. 1. Note that we do not exhibit the diagrams, which are equivalent under exchange of the u and d quarks. It will be observed that nonfactorizable diagrams, especially those with both the charm quarks in the J/ψ meson attached by the hard gluons, dominate. The vertex corrections to the four-fermion operators, which are calculated in the improved QCD factorization [19–21], are of higher orders in the PQCD approach and not considered in the present leading-order formalism.

A naive power counting for the $\Lambda_b \to \Lambda J/\psi$ decay indicates that the important kinematic region corresponds to the parton longitudinal and transverse momenta of $O(\bar{\Lambda})$. This is the reason each diagram for this mode is characterized by the scale $\bar{\Lambda}$ as stated in the Introduction. The factorizable contributions, characterized by this low scale, are suppressed by the small Wilson coefficient $a_2 = C_2 + C_1/N_c$, N_c being the number of colors. The $\Lambda_b \to \Lambda J/\psi$ decay is then dominated by the nonfactorizable contributions as in the $B \to J/\psi K^{(*)}$ decays. Since the J/ψ meson is a color-singlet object with the two valence quarks moving parallelly, there exists soft cancellation in a pair of nonfactorizable diagrams [22] such as Figs. 1(f) and 1(h). Hence, the parton momenta in the Λ baryon become of $O(M_{\Lambda_b}[1-(M_{J/\psi}/M_{\Lambda_b})^2])$, and the $\Lambda_b \to \Lambda J/\psi$ decay is characterized by the larger scale $\sqrt{\bar{\Lambda} M_{\Lambda_b}[1-(M_{J/\psi}/M_{\Lambda_b})^2]}$. It then makes sense to apply PQCD to this heavy-to-heavy decay mode.

At last, the $\Lambda_b \to \Lambda J/\psi$ decay amplitudes are expressed as the convolution of the above factors,

$$C(t) \otimes H(t) \otimes g(t,b) \otimes \exp[-s(P,b)] \otimes \phi(x,b) \ . \tag{4}$$

All the convolution factors, except $\phi(x,b)$, are calculable. The hadron distribution amplitude $\phi(x,b)$, though not calculable, are universal, since they absorb long-distance dynamics of a decay process, which is insensitive to short-distance dynamics involved in the b quark decays. Based on universality, we employ the hadron distribution amplitudes extracted from other experimental data or from QCD sum rules to make predictions for the $\Lambda_b \to \Lambda J/\psi$ decay. Note that the hard scale t is a convolution variable, since the derivation of Eq. (4) starts with the eight-quark, instead of four-quark, amplitudes. Its precise expression should be determined by diminishing next-to-leading-order corrections to the hard amplitude $H(t)$. In this work we shall consider the different choices of t as the main source of the theoretical uncertainty.

III. DISTRIBUTION AMPLITUDES

We define kinematics of the initial and final hadrons as follows. The Λ_b baryon is assumed to be at rest, and the Λ baryon, regarded as being massless, recoils in the minus direction. The momenta p, p' and $q = p - p'$ of the Λ_b baryon, the Λ baryon and the J/ψ meson, respectively, and the momenta of their valence quarks are parametrized as

$$\begin{aligned}
&p = (p^+, p^-, \mathbf{0}) = \frac{M_{\Lambda_b}}{\sqrt{2}}(1,1,\mathbf{0}) \ , \\
&k_1 = (x_1 p^+, p^-, \mathbf{k}_{1T}) \ , \quad k_2 = (x_2 p^+, 0, \mathbf{k}_{2T}) \ , \quad k_3 = (x_3 p^+, 0, \mathbf{k}_{3T}) \ , \\
&p' = (0, p'^-, \mathbf{0}) = (0, \rho p^-, \mathbf{0}) \ , \\
&k'_1 = (0, x'_1 p'^-, \mathbf{k}'_{1T}) \ , \quad k'_2 = (0, x'_2 p'^-, \mathbf{k}'_{2T}) \ , \quad k'_3 = (0, x'_3 p'^-, \mathbf{k}'_{3T}) \ , \\
&q = (q^+, q^-, \mathbf{0}) = (p^+, r^2 p^-, \mathbf{0}) \ , \\
&q_1 = (y q^+, y q^-, \mathbf{q}_T) \ , \quad q_2 = ((1-y)q^+, (1-y)q^-, -\mathbf{q}_T) \ ,
\end{aligned} \tag{5}$$

with the constants,

$$\rho = 1 - r^2 \ , \quad r = \frac{M_{J/\psi}}{M_{\Lambda_b}} \ . \tag{6}$$

k_1 (k'_1) is the b (s) quark momentum, x_i (x'_i) are the momentum fractions associated with the Λ_b (Λ) baryon, and $\mathbf{k}_T^{(\prime)}$ the corresponding transverse momenta, satisfying $\sum_l \mathbf{k}_{lT}^{(\prime)} = 0$. y is the momentum fraction and $\mathbf{q}_T$ the transverse momenta carried by the charm quark in the J/ψ meson.

The structure of the Λ_b baryon wave function Y_{Λ_b} is simplified under the assumptions that the spin and orbital degrees of freedom of the light quark system are decoupled, and that the Λ_b baryon is in the ground state (s-wave). The wave function is given, in the transverse momentum space, by [23]

$$\begin{aligned}
(Y_{\Lambda_b})_{\alpha\beta\gamma}(k_i,\mu) &= \frac{1}{2\sqrt{2}N_c}\int \prod_{l=2}^{3} \frac{dw_l^- d\mathbf{w}_l}{(2\pi)^3} e^{ik_l\cdot w_l} \epsilon^{abc} \langle 0|T[b_\alpha^a(0) u_\beta^b(w_2) d_\gamma^c(w_3)]|\Lambda_b(p)\rangle \ , \\
&= \frac{f_{\Lambda_b}}{8\sqrt{2}N_c}[(\not{p} + M_{\Lambda_b})\gamma_5 C]_{\beta\gamma}[\Lambda_b(p)]_\alpha \Psi(k_i,\mu) \ ,
\end{aligned} \tag{7}$$

where b, u, and d are the quark fields, a, b, and c the color indices, α, β, and γ the spinor indices, C the charge conjugation matrix, $\Lambda_b(p)$ the Λ_b baryon spinor, and f_{Λ_b} the normalization constant.

The Λ baryon wave functions are defined, in the transverse momentum space, via

$$
\begin{aligned}
(Y_\Lambda)_{\alpha\beta\gamma}(k'_i,\mu) &= \frac{1}{2\sqrt{2}N_c}\int\prod_{l=2}^{3}\frac{dw_l^+ d\mathbf{w}_l}{(2\pi)^3}e^{ik'_l\cdot w_l}\epsilon^{abc}\langle 0|T[s^a_\alpha(0)u^b_\beta(w_2)d^c_\gamma(w_3)]|\Lambda(p')\rangle\ , \\
&= \frac{f_\Lambda}{8\sqrt{2}N_c}\left\{(\not{p}'C)_{\beta\gamma}[\gamma_5\Lambda(p')]_\alpha\Phi^V(k'_i,\mu) + (\not{p}'\gamma_5 C)_{\beta\gamma}[\Lambda(p')]_\alpha\Phi^A(k'_i,\mu)\right\} \\
&\quad -\frac{f_\Lambda^T}{8\sqrt{2}N_c}(\sigma_{\mu\nu}p'^{\nu}C)_{\beta\gamma}[\gamma^\mu\gamma_5\Lambda(p')]_\alpha\Phi^T(k'_i,\mu)\ ,
\end{aligned}
\tag{8}
$$

with the normalization constants f_Λ and f_Λ^T, the Λ baryon spinor $\Lambda(p')$, and the definition $\sigma_{\mu\nu} = [\gamma_\mu,\gamma_\nu]/2$. The wave functions Φ^V, Φ^A, and Φ^T are associated with the different spin structures of the three valence quarks in the Λ baryon.

The J/ψ meson wave function is expressed as

$$
\begin{aligned}
(Y_{J/\psi})_{\alpha\beta}(q_i,\lambda,\mu) &= \frac{1}{N_c}\int\frac{d^4w}{(2\pi)^4}e^{iq_1\cdot w}\langle 0|T[\bar{c}_\beta(0)c_\alpha(w)]|J/\psi(q,\lambda)\rangle \\
&= \frac{1}{\sqrt{2N_c}}[\not{\epsilon}(q,\lambda)(\not{q}+M_{J/\psi})]_{\alpha\beta}\,\Pi(q_i,\mu)\ ,
\end{aligned}
\tag{9}
$$

where the J/ψ meson decay constant $f_{J/\psi}$ has been absorbed into the wave function Π, and $\epsilon_\mu(q,\lambda)$ is the polarization vector of the J/ψ meson with the helicity λ. It has been assumed that the J/ψ meson wave functions associated with longitudinal and transverse polarizations possess the same form in the above expression. To ensure that the valence charm quarks are close to the mass shell, Π should have a sharp peak at $y \sim 1/2$. The J/ψ meson wave function has been determined from the data of the $B \to J/\psi K^{(*)}$ decays [7]. For the factorizable amplitudes, the momentum fraction y is integrated out, and only the decay constant $f_{J/\psi}$ is relevant.

When the transverse degrees of freedom of partons are taken into account, the factorization of a QCD process should be constructed in the b space [16], with b being the variable conjugate to k_T. This is the reason $1/b$ serves as the factorization scale stated in Sec. II. Sudakov resummation of the double logarithms and RG summations of the single logarithms contained in the above hadron wave functions lead to

$$
\begin{aligned}
\Psi(k_i^+,b_i,\mu) &= \exp\left[-\sum_{l=2}^{3}s(w,k_l^+) - 3\int_w^\mu\frac{d\bar\mu}{\bar\mu}\gamma(\alpha_s(\bar\mu))\right]\psi(x_i)\ , \\
\Phi^j(k'^-_i,b'_i,\mu) &= \exp\left[-\sum_{l=1}^{3}s(w',k'^-_l) - 3\int_{w'}^\mu\frac{d\bar\mu}{\bar\mu}\gamma(\alpha_s(\bar\mu))\right]\phi^j(x_i)\ , \\
\Pi(q_i^+,b_q,\mu) &= \exp\left[-\sum_{l=1}^{2}s(w_q,q_l^+) - 2\int_{w_q}^\mu\frac{d\bar\mu}{\bar\mu}\gamma(\alpha_s(\bar\mu))\right]\pi(y)\ ,
\end{aligned}
\tag{10}
$$

with the superscript $j = V$, A and T, and the quark anomalous dimension $\gamma = -\alpha_s/\pi$. The Sudakov exponent s for the J/ψ meson depends on the dominant component q_l^+. The factorization scales w, w' and w_q are chosen as

$$
w = \min\left(\frac{1}{b_1},\frac{1}{b_2},\frac{1}{b_3}\right)\ ,\quad w' = \min\left(\frac{1}{b'_1},\frac{1}{b'_2},\frac{1}{b'_3}\right)\ ,\quad w_q = \frac{1}{b_q}\ ,
\tag{11}
$$

with the variables,

$$
b_1 = |\mathbf{b}_2 - \mathbf{b}_3|\ ,\quad b'_1 = |\mathbf{b}'_2 - \mathbf{b}'_3|\ .
\tag{12}
$$

The initial conditions ψ, ϕ^j and π of the Sudakov evolution absorb nonperturbative dynamics below the factorization scales w, w' and w_q, respectively. Note that the Sudakov effect from the J/ψ meson is weak, since the distribution amplitude $\pi(y,\lambda)$ vanishes rapidly as $y \to 0, 1$.

The explicit expression of the Sudakov exponent s is given by

$$
s(w,Q) = \int_w^Q\frac{dp}{p}\left[\ln\frac{Q}{p}A(\alpha_s(p)) + B(\alpha_s(p))\right]\ ,
\tag{13}
$$

where the anomalous dimensions A to two loops and B to one loop are

$$\begin{aligned} A &= C_F\frac{\alpha_s}{\pi}+\left[\frac{67}{9}-\frac{\pi^2}{3}-\frac{10}{27}n_f+\frac{8}{3}\beta_0\ln\frac{e^{\gamma_E}}{2}\right]\left(\frac{\alpha_s}{\pi}\right)^2 , \\ B &= \frac{2}{3}\frac{\alpha_s}{\pi}\ln\frac{e^{2\gamma_E-1}}{2} , \end{aligned} \tag{14}$$

$C_F=\frac{4}{3}$ being a color factor, $n_f=4$ the flavor number, and γ_E the Euler constant. The one-loop running coupling constant,

$$\frac{\alpha_s(\mu)}{\pi}=\frac{1}{\beta_0\ln(\mu^2/\Lambda^2_{\rm QCD})} , \tag{15}$$

with the coefficient $\beta_0=(33-2n_f)/12$, will be substituted into Eq. (13).

IV. FACTORIZATION FORMULAS

The $\Lambda_b\to J/\psi\Lambda$ decay amplitude $\mathcal{M}$ is expressed as

$$\mathcal{M}=i\sum_\lambda\mathcal{M}(\lambda) , \tag{16}$$

where the amplitude $\mathcal{M}(\lambda)$ can be decomposed into different structures with the corresponding coefficients A_1, A_2, B_1, and B_2:

$$\mathcal{M}(\lambda)=\bar\Lambda(p')\left[A_1\not\epsilon\gamma_5+A_2\frac{p\cdot\epsilon}{M_{\Lambda_b}}\gamma_5+B_1\not\epsilon+B_2\frac{p\cdot\epsilon}{M_{\Lambda_b}}\right]\Lambda_b(p) . \tag{17}$$

The general factorization formula for $\mathcal{M}(\lambda)$ is written as

$$\begin{aligned} \mathcal{M}(\lambda) = {} & \frac{G_F}{\sqrt{2}}V_{cb}V^*_{cs}\int[\mathcal{D}x]\int[\mathcal{D}b](\bar{Y}_\Lambda)_{\alpha'\beta'\gamma'}(p',x',b',\mu) \\ & \times(Y_{J/\psi})^\dagger_{\rho\rho'}(q,y,b_q,\lambda,\mu)\,\mathcal{H}^{\alpha'\beta'\gamma'\rho'\alpha\beta\gamma\rho}(x,x',y,b,b',b_q,M_{\Lambda_b},\mu)\,(Y_{\Lambda_b})_{\alpha\beta\gamma}(p,x,b,\mu) , \end{aligned} \tag{18}$$

with the measure of the momentum fractions,

$$[\mathcal{D}x]=[dx][dx']dy , \quad [dx]=dx_1dx_2dx_3\delta\left(1-\sum_{l=1}^3x_l\right) , \quad [dx']=dx'_1dx'_2dx'_3\delta\left(1-\sum_{l=1}^3x'_l\right) . \tag{19}$$

The measure of the transverse extents $[\mathcal{D}b]$ will be defined in Appendix A.

The RG analysis of $\mathcal{H}$ leads to

$$\begin{aligned} \mathcal{H}(x,x',y,b,b',b_q,M_{\Lambda_b},\mu) = {} & \exp\left[-n\int_\mu^t\frac{d\bar\mu}{\bar\mu}\gamma(\alpha_s(\bar\mu))\right] \\ & \times\mathcal{H}(x,x',y,b,b',b_q,M_{\Lambda_b},t) , \end{aligned} \tag{20}$$

with the integer $n=6$ for the factorizable diagrams and $n=8$ for the nonfactorizable diagrams. The superscripts α', β', $\cdots$, have been suppressed. The argument t in the initial condition of $\mathcal{H}$ implies that the Wilson coefficient and the running coupling constants α_s for the hard gluons are evaluated at t. This initial condition will be calculated based on the lowest-order diagrams in Fig. 1. For the purpose of presentation, we shall rewrite the initial hard amplitude as $\mathcal{H}=aH_F\Omega$, where a is the Wilson coefficient, H_F the numerator of $\mathcal{H}$ depending on the spin structure of the three valence quarks in the Λ baryon, and Ω the Fourier transformation of the denominator of $\mathcal{H}$ from the k_T space to the b space.

Substituting Eqs. (10) and (20) into Eq. (18), we derive the factorization formulas,

$$\begin{aligned} F^i = {} & 2G_FV_{cb}V^*_{cs}\sum_{j=V,A,T}\frac{\pi^2}{54\sqrt{3}}f_{\Lambda_b}f^j_\Lambda\int[\mathcal{D}x]\int[\mathcal{D}b]^i[\alpha_s(t^i)]^2a^i(t^i) \\ & \times\psi(x)\phi^j(x')\pi(y)\exp[-S^i]H^{ij}_F\Omega^i , \end{aligned} \tag{21}$$

where F represents the coefficients A_1, A_2, B_1, and B_2, the superscript i labels the diagrams in Fig. 1, and the superscript j labels V, A, and T associated with the spin structures of the valence quarks in the Λ baryon. The factor 2 comes from the symmetry under the u-d exchange. The Wilson coefficients are $a^i = C_1/N_c$ for the nonfactorizable diagrams with only one hard gluon attaching the c quark or the $\bar{c}$ quark, and $a^i = a_2 = C_2 + C_1/N_c$ for the factorizable diagrams and for the nonfactorizable diagrams with two hard gluon attaching the two quarks of the J/ψ meson. At the characteristic scale of order $\sqrt{\bar{\Lambda} M_{\Lambda_b}[1-(M_{J/\psi}/M_{\Lambda_b})^2]}$, C_1/N_c is about few times larger than a_2. The Fourier integrals employed in this work, and the resultant measures $[\mathcal{D}b]^i$ of the transverse extents for each diagram i are given in Appendix A. The explicit expressions of Ω^i are presented in Appendix B. The functions H_F^{ij} are given in Appendix C. To derive the expressions of H_F^{ij}, we have chosen $x_1 = 1$ and $x_2 = x_3 = 0$, since x_2 and x_3, being of $O(\bar{\Lambda}/m_b)$, are negligible in the current leading-power analysis.

The main theoretical uncertainty of our predictions come from higher-order corrections to the hard amplitudes, which can be reflected by the choice of the hard scale t^i [22,24]. We shall consider the following two choices:

$$\begin{aligned} t^i &= \max(t_1^i, t_2^i, w, w', w_q) \ , \\ t^i &= \max\left(\frac{t_1^i + t_2^i}{2}, w, w', w_q\right) \ , \end{aligned} \tag{22}$$

where the hard scales t_1^i and t_2^i associated with the two hard gluons in each diagram i are listed in Table I. The max in the above expressions simply means that the hard scales should be larger than the factorization scales. It is expected that the first choice will lead to values lower than those from the second one. The theoretical uncertainty can be reduced after next-to-leading-order corrections are included.

The exponents S^i are given by

$$\begin{aligned} S^i &= \sum_{l=2}^{3} s(w, x_l p^+) + 3\int_w^{t^i} \frac{d\bar{\mu}}{\bar{\mu}} \gamma(\alpha_s(\bar{\mu})) \\ &\quad + \sum_{l=1}^{3} s(w', x_l' p'^-) + 3\int_{w'}^{t^i} \frac{d\bar{\mu}}{\bar{\mu}} \gamma(\alpha_s(\bar{\mu})) \ , \end{aligned} \tag{23}$$

$$\begin{aligned} S^i &= \sum_{l=2}^{3} s(w, x_l p^+) + 3\int_w^{t^i} \frac{d\bar{\mu}}{\bar{\mu}} \gamma(\alpha_s(\bar{\mu})) \\ &\quad + \sum_{l=1}^{3} s(w', x_l' p'^-) + 3\int_{w'}^{t^i} \frac{d\bar{\mu}}{\bar{\mu}} \gamma(\alpha_s(\bar{\mu})) \\ &\quad + \sum_{l=1}^{2} s(w_q, y_l q^+) + 2\int_{w_q}^{t^i} \frac{d\bar{\mu}}{\bar{\mu}} \gamma(\alpha_s(\bar{\mu})) \ , \end{aligned} \tag{24}$$

for the factorizable and nonfactorizable diagrams, respectively. The Sudakov exponential associated the J/ψ meson distribution amplitude appear only in the nonfactorizable diagrams. The evolution factors described by γ correspond to $g(t, b)$ introduced in Sec. II.

V. NUMERICAL RESULTS

In this section we evaluate the factorization formulas in Eq. (21) numerically. For the Λ_b baryon distribution amplitude ψ, we adopt the model proposed in [25],

$$\psi(x_1, x_2, x_3) = N x_1 x_2 x_3 \exp\left[-\frac{M_{\Lambda_b}^2}{2\beta^2 x_1} - \frac{m_l^2}{2\beta^2 x_2} - \frac{m_l^2}{2\beta^2 x_3}\right] \ , \tag{25}$$

where the shape parameter $\beta = 1.0$ GeV, and the mass of light degrees of freedom in the Λ_b baryon, $m_l = 0.3$ GeV, have been determined in [2]. The normalization

$$\int [dx] \psi(x_1, x_2, x_3) = 1 \ , \tag{26}$$

leads to the constant $N = 6.67 \times 10^{12}$. The constant $f_{\Lambda_b} = 2.71 \times 10^{-3}$ GeV^2 and the above Λ_b baryon distribution amplitude ψ have been chosen to satisfy the experimental upper bound of the $\Lambda_b \to \Lambda_c l \bar{\nu}$ branching ratio and the heavy quark symmetry [2].

The Λ baryon distribution amplitudes have been derived using QCD sum rules [11,12]. The asymmetric distribution in the momentum fractions of the three quarks implies $SU(3)$ symmetry breaking [12]. In this work we adopt the models proposed in [11],

$$\begin{aligned}
\phi^V(x_1,x_2,x_3) &= 42\,\phi_{as}(x_1,x_2,x_3)\left[0.111(x_3^2-x_2^2)+0.093(x_2-x_3)\right] \;, \\
\phi^A(x_1,x_2,x_3) &= -42\phi_{as}(x_1,x_2,x_3)\left[0.093(x_2^2+x_3^2)+0.376x_1^2\right. \\
&\quad \left. -0.194x_2x_3-0.207x_1(x_2+x_3)\right] \;, \\
\phi^T(x_1,x_2,x_3) &= 42\,\phi_{as}(x_1,x_2,x_3)\left[3.6(x_2^2-x_3^2)+0.32(x_2-x_3)\right] \;,
\end{aligned} \tag{27}$$

with the asymptotic distribution amplitude,

$$\phi_{as}(x_1,x_2,x_3) = 120\,x_1x_2x_3 \;. \tag{28}$$

The normalization constants f_Λ and f_Λ^T are chosen as

$$f_\Lambda \;=\; 0.45\times 10^{-2}\ \mathrm{GeV}^2 \;, \quad f_\Lambda^T \;=\; 0.2\times 10^{-2}\ \mathrm{GeV}^2 \;. \tag{29}$$

It is easy to observe that the above Λ baryon distribution amplitudes satisfy the relations,

$$\begin{aligned}
\phi^V(x_1,x_2,x_3) &= -\phi^V(x_1,x_3,x_2) \;, \\
\phi^A(x_1,x_2,x_3) &= \phi^A(x_1,x_3,x_2) \;, \\
\phi^T(x_1,x_2,x_3) &= -\phi^T(x_1,x_3,x_2) \;,
\end{aligned} \tag{30}$$

and the normalization,

$$\int [dx]\phi^{V,A,T}(x_1,x_2,x_3) = 1 \;. \tag{31}$$

It is most likely that the two charm quarks in the J/ψ meson carry the equal fractional momenta, such that they are close to the mass shell. Hence, the following J/ψ meson distribution amplitudes with sharp peaks at the momentum fraction $y = 1/2$ have been proposed [7],

$$\pi(y) = \frac{5\sqrt{6}}{2}\, f_{J/\psi}\, y^2(1-y)^2 \;, \tag{32}$$

with the J/ψ meson decay constant $f_{J/\psi} = 390$ MeV [26]. It has been found that Eq. (32) gives the branching ratios $B(B \to J/\psi K^{(*)})$ in agreement with experimental data [7]. We have confirmed that the PQCD predictions are not sensitive to the functional form of π, as long as it has a sharp peak at $y \sim 1/2$.

Employing the parameters $G_F = 1.16 \times 10^{-5}$ GeV^{-2}, $V_{cb} = 0.04$ and $V_{cs} = 0.975$, $\Lambda_{\rm QCD} = 0.2$ GeV, and the masses $M_{\Lambda_b} = 5.624$ GeV and $M_{J/\psi} = 3.097$ GeV, we obtain the coefficients A_1, A_2, B_1, and B_2. The contributions from the transverse component ϕ^T of the Λ baryon distribution amplitudes are listed in Table II. These coefficients, dominated by the nonfactorizable amplitudes, are mainly imaginary. The $\Lambda_b \to \Lambda J/\psi$ decay rate is written as

$$\Gamma = \frac{1}{8\pi}\frac{p_c}{M_{\Lambda_b}^2}|\mathcal{M}|^2 \;, \tag{33}$$

where p_c is the magnitude of either of the final-state particle momentum in the center-of-mass frame. Following the choices of the hard scale t in Eq. (22), we derive the branching ratio,

$$B(\Lambda_b \to \Lambda J/\psi) = (1.7 \sim 5.3)\times 10^{-4} \;, \tag{34}$$

for the Λ_b baryon lifetime $\tau = (1.24 \pm 0.08)\times 10^{-12}$ s. Here we do not consider the minor uncertainty from τ. The value in Eq. (34) is consistent with the experimental data [27],

$$B(\Lambda_b \to \Lambda J/\psi) = (4.7 \pm 2.8)\times 10^{-4} \;. \tag{35}$$

We also calculate the asymmetry parameter α associated with the anisotropic angular distribution of the Λ baryons emitted in polarized Λ_b baryon decays:

$$d\Gamma \propto (1 + \alpha p' \cdot \mathcal{P}) \;, \tag{36}$$

$\mathcal{P}$ being the Λ_b baryon polarization. The explicit expression of α is given by [13]

$$\alpha = \frac{4M_{J/\psi}^2 Re(S^* P_2) + 2E_{J/\psi}^2 Re[(S+D)^* P_1]}{2(|S|^2 + |P_2|^2)M_{J/\psi}^2 + (|S+D|^2 + |P_1|^2)E_{J/\psi}^2} \;, \tag{37}$$

with the factors,

$$\begin{aligned} S &= -A_1 \;, \\ D &= -\frac{p_c^2}{E_{J/\psi}(E_\Lambda + M_\Lambda)}(A_1 - A_2) \;, \\ P_1 &= -\frac{p_c}{E_{J/\psi}}\left[\frac{M_{\Lambda_b} + M_\Lambda}{E_\Lambda + M_\Lambda}B_1 + B_2\right] \;, \\ P_2 &= \frac{p_c}{E_\Lambda + M_\Lambda}B_1 \;, \end{aligned} \tag{38}$$

where $E_{J/\psi}$ (E_Λ) is the energy of the J/ψ meson (Λ baryon), and the Λ baryon mass M_Λ has been set to zero for consistency. The result is, following Eq. (22),

$$\alpha = -0.17 \sim -0.14 \;, \tag{39}$$

consistent with those derived from the quark model based on FA [28,29] shown in Table III. The predictions for α are very stable with respect to the variation of the hard scale t and of the hadron distribution amplitudes. Therefore, it serves as an ideal quantity to test the PQCD approach.

VI. CONCLUSION

In this paper we have analyzed the nonleptonic heavy baryon decay $\Lambda_b \to \Lambda J/\psi$ using the PQCD formalism. It is a special heavy-to-heavy mode, to which PQCD is applicable, because of the soft cancellation between a pair of nonfactorizable diagrams. We have shown that nonfactorizable contributions dominate in this mode, similar to the heavy meson cases $B \to J/\psi K^{(*)}$, since factorizable contributions are suppressed by the small Wilson coefficient a_2. After considering the theoretical uncertainty arising from higher-order corrections, we have derived the branching ratio $B(\Lambda_b \to \Lambda J/\psi)$ and the asymmetry parameter α associated with the anisotropic angular distribution of the Λ baryons produced in the polarized Λ_b baryon decays. The latter quantity is stable with respect to the variation of the hadron distribution amplitudes and to higher-order corrections. The comparison of our predictions with the experimental data will provide a test of the PQCD formalism.

The PQCD results are consistent with those derived from other approaches based on FA as indicated in Table III. However, we emphasize that the theoretical bases between PQCD and FA are very different. In PQCD, a_2 is a Wilson coefficient, which is small in a wide range of the energy scale. To explain the experimental data, large nonfactorizable contributions are necessary. In FA nonfactorizable contributions are neglected. To account for the data, a_2 must be treated as a free parameter, and the value $a_2 \sim 0.23$ [13] has been adopted. Also, nonfactorizable contributions are imaginary and their strong phases can be evaluated in PQCD, while the parameter a_2 is real (or with an arbitrary phase) in FA. As stressed in [30], the imaginary nonfactorizable amplitudes determine the relative phases of the various $B \to D\pi$ decay modes, which are essential for explaining the recent $\bar{B}_d \to D^{(*)0}\pi^0$ data [31,32].

This work was supported by the National Science Council of R.O.C. under Grant Nos. NSC-90-2112-M-001-077, NSC-90-2811-M-001-042 and NSC-90-2112-M-001-038.

APPENDIX A: FOURIER INTEGRATIONS AND B MEASURES

We list below the Fourier integration formulas that have been employed in the derivation of the hard amplitudes in the b space, where J_1, N_1, K_0 and K_1 are the Bessel functions, and z_i the Feynman parameters:

$$\int d^2k \frac{e^{i\mathbf{k}\cdot\mathbf{b}}}{k^2+A} = 2\pi K_0(\sqrt{A}b) \;, \quad A \, > \, 0 \;, \tag{A1}$$

$$\int d^2k \frac{e^{i\mathbf{k}\cdot\mathbf{b}}}{(k^2+A)(k^2+B)} = \pi \int_0^1 dz \frac{K_1(\sqrt{Z_1}|b|)}{\sqrt{Z_1}} \;, \quad A,\, B \, > \, 0 \;, \tag{A2}$$

$$\begin{aligned}
&\int d^2k_1 d^2k_2 \frac{e^{i(\mathbf{k}_1\cdot\mathbf{b}_1+\mathbf{k}_2\cdot\mathbf{b}_2)}}{(k_1^2+A)(k_2^2+B)[(k_1+k_2)^2+C]} \\
=\pi^2 &\int_0^1 \frac{dz_1 dz_2}{z_1(1-z_1)} \frac{\sqrt{X_2}}{\sqrt{|Z_2|}} \Bigg\{ K_1(\sqrt{X_2 Z_2})\theta(Z_2) \\
&+\frac{\pi}{2}\left[N_1(\sqrt{X_2|Z_2|}) - iJ_1(\sqrt{X_2|Z_2|})\right]\theta(-Z_2)\Bigg\} \;, \\
&A \, > \, 0 \;, \text{ and } B,\; C \text{ arbitrary} \;,
\end{aligned} \tag{A3}$$

$$\begin{aligned}
&\int d^2k_1 d^2k_2 d^2k_3 \frac{e^{i(\mathbf{k}_1\cdot\mathbf{b}_1+\mathbf{k}_2\cdot\mathbf{b}_2+\mathbf{k}_3\cdot\mathbf{b}_3)}}{(k_1^2+A)(k_2^2+B)(k_3^2+C)[(k_1+k_2+k_3)^2+D]} \\
=\pi^3 &\int_0^1 \frac{dz_1 dz_2 dz_3}{z_1(1-z_1)z_2(1-z_2)} \frac{\sqrt{X_3}}{\sqrt{|Z_3|}} \Bigg\{ K_1(\sqrt{X_3 Z_3})\theta(Z_3) \\
&+\frac{\pi}{2}\left[N_1(\sqrt{X_3|Z_3|}) - iJ_1(\sqrt{X_3|Z_3|})\right]\theta(-Z_3)\Bigg\} \;, \\
&A,\; B \, > \, 0 \;, \text{ and } C,\; D \text{ arbitrary} \;,
\end{aligned} \tag{A4}$$

with the variables,

$$Z_1 = A\, z + B\,(1-z) \;, \tag{A5}$$

$$\begin{aligned}
Z_2 &= A\,(1-z_2) + \frac{z_2}{z_1(1-z_1)}[B\,(1-z_1) + C\, z_1] \;, \\
X_2 &= (b_1 - z_1 b_2)^2 + \frac{z_1(1-z_1)}{z_2} b_2^2 \;,
\end{aligned} \tag{A6}$$

$$\begin{aligned}
Z_3 &= A\,(1-z_3) + \frac{z_3}{z_2(1-z_2)}\left\{B\,(1-z_2) + \frac{z_2}{z_1(1-z_1)}[C\,(1-z_1) + D\, z_1]\right\} \;, \\
X_3 &= [b_1 - b_2 z_2 - b_3 z_2(1-z_1)]^2 + \frac{z_2(1-z_2)}{z_3}(b_2 - b_3 z_1)^2 \\
&+ \frac{z_1(1-z_1)z_2(1-z_2)}{z_2 z_3} b_3^2 \;.
\end{aligned} \tag{A7}$$

After performing the above integrations, we combine the z measures with the ordinary b measures,

$$[db_l] = \frac{d^2 b_l}{(2\pi)^2} \;, \tag{A8}$$

to form the special b measures $[\mathcal{D}b]$ appearing in Eq. (21). $[\mathcal{D}b]^i$ for each diagram i in Fig. 1 is given by

$$[\mathcal{D}b]^{(a)} = [\mathcal{D}b]^{(j)} = (2\pi)^3 [db_2][db_2'][db_3'] dz_1 dz_2 \;, \tag{A9}$$

$$[\mathcal{D}b]^{(b)} = [\mathcal{D}b]^{(c)} = [\mathcal{D}b]^{(g)} = [\mathcal{D}b]^{(i)} = [\mathcal{D}b]^{(m)} = [\mathcal{D}b]^{(n)} = [\mathcal{D}b]^{(o)} = [\mathcal{D}b]^{(p)} = (2\pi)^4 [db_2][db_2'][db_3'][db_q] \;, \tag{A10}$$

$$[\mathcal{D}b]^{(d)} = (2\pi)^3[db_2][db_2'][db_3']dz_1 \ , \tag{A11}$$

$$[\mathcal{D}b]^{(e)} = [\mathcal{D}b]^{(h)} = (2\pi)^3[db_2'][db_3'][db_q]dz_1dz_2 \ , \tag{A12}$$

$$[\mathcal{D}b]^{(f)} = (2\pi)^3[db_2'][db_3'][db_q]dz_1dz_2dz_3 \ , \tag{A13}$$

$$[\mathcal{D}b]^{(k)} = [\mathcal{D}b]^{(l)} = [\mathcal{D}b]^{(q)} = [\mathcal{D}b]^{(r)} = (2\pi)^4[db_2][db_3][db_2'][db_3'] \ . \tag{A14}$$

APPENDIX B: EXPRESSIONS OF Ω^I

Employing the integration formulas in Appendix A, we derive the hard amplitudes in the b space. The hard function Ω^i for each diagram i in Fig. 1, which arises from Fourier transformation of the denominators of the internal particle propagators, is expressed as

$$\Omega^{(a)} = \frac{1}{4z_1(1-z_1)}\frac{\sqrt{B_a}}{\sqrt{Z_a}}K_0\left(\sqrt{x_3x_3'\rho}M_{\Lambda_b}b_3'\right)K_1\left(\sqrt{Z_aB_a}\right) \ , \tag{B1}$$

with

$$\begin{aligned} B_a &= \frac{z_1(1-z_1)}{z_2}(b_2-b_2')^2 + [(1-z_1)b_2 + z_1b_2']^2 \ , \\ Z_a &= x_2x_2'\rho M_{\Lambda_b}^2(1-z_2) + \frac{z_2}{z_1(1-z_1)}[(1-x_1)z_1 + x_3(1-x_2')(1-z_1)]\rho M_{\Lambda_b}^2 \ , \end{aligned} \tag{B2}$$

$$\begin{aligned} \Omega^{(b)} = &K_0\left(\sqrt{x_2x_2'\rho}M_{\Lambda_b}(b_2+b_q)\right)K_0\left(\sqrt{x_3x_3'\rho}M_{\Lambda_b}b_3'\right) \\ &\times K_0\left(\sqrt{x_3(1-x_2')\rho}M_{\Lambda_b}|b_2-b_2'|\right)\left\{K_0\left(\sqrt{Z_b}M_{\Lambda_b}b_q\right)\ \theta(Z_b)\right. \\ &\left.+\frac{\pi}{2}\left[-N_0\left(\sqrt{|Z_b|}M_{\Lambda_b}b_q\right) + iJ_0\left(\sqrt{|Z_b|}M_{\Lambda_b}b_q\right)\right]\ \theta(-Z_b)\right\} \ , \end{aligned} \tag{B3}$$

with

$$Z_b = \frac{r^2}{4} - (1-x_2-y)[x_2'\rho + (1-y)r^2] \ , \tag{B4}$$

$$\begin{aligned} \Omega^{(c)} = &K_0\left(\sqrt{x_2x_2'\rho}M_{\Lambda_b}|b_2-b_q|\right)K_0\left(\sqrt{x_3x_3'\rho}M_{\Lambda_b}b_3'\right) \\ &\times K_0\left(\sqrt{x_3(1-x_2')\rho}M_{\Lambda_b}|b_2-b_2'|\right)\left\{K_0\left(\sqrt{Z_c}M_{\Lambda_b}b_q\right)\ \theta(Z_c)\right. \\ &\left.+\frac{\pi}{2}\left[-N_0\left(\sqrt{|Z_c|}M_{\Lambda_b}b_q\right) + iJ_0\left(\sqrt{|Z_c|}M_{\Lambda_b}b_q\right)\right]\ \theta(-Z_c)\right\} \ , \end{aligned} \tag{B5}$$

with

$$Z_c = \frac{r^2}{4} + (x_2-y)[x_2'\rho + (1-y)r^2] \ , \tag{B6}$$

$$\Omega^{(d)} = \frac{1}{2\sqrt{Z_d}}K_0\left(\sqrt{x_2x_2'\rho}M_{\Lambda_b}b_2\right)K_0\left(\sqrt{x_3x_3'\rho}M_{\Lambda_b}b_3'\right)K_1\left(\sqrt{Z_d}M_{\Lambda_b}|b_2-b_2'|\right) \ , \tag{B7}$$

with

$$Z_d = [x_3 + x_2'(1-x_3)\rho] M_{\Lambda_b}^2 z_1 + x_3(1-x_2')\rho M_{\Lambda_b}^2 (1-z_1) \ , \tag{B8}$$

$$\begin{aligned}\Omega^{(e)} = {} & \frac{1}{4z_1(1-z_1)} \frac{\sqrt{B_e}}{\sqrt{|Z_e|}} K_0\left(\sqrt{x_3 x_3' \rho} M_{\Lambda_b}(b_3' + b_q)\right) \left\{ K_1\left(\sqrt{Z_e B_e}\right)\ \theta(Z_e) \right. \\ & \left. + \frac{\pi}{2}\left[N_1\left(\sqrt{|Z_e| B_e}\right) - iJ_1\left(\sqrt{|Z_e| B_e}\right)\right]\ \theta(-Z_e) \right\} ,\end{aligned} \tag{B9}$$

with

$$\begin{aligned}B_e = {} & \frac{z_1(1-z_1)}{z_2} b_q^2 + (b_2' + z_1 b_q)^2 \ , \\ Z_e = {} & x_2 x_2' \rho M_{\Lambda_b}^2 (1-z_2) + \frac{z_2}{z_1(1-z_1)} \left\{ \left[\frac{r^2}{4} - (x_1 - y)(1 - x_1'\rho - y r^2)\right] z_1 \right. \\ & \left. + \left[\frac{r^2}{4} - (1 - x_3 - y)(x_3'\rho + (1-y) r^2)\right] (1-z_1) \right\} M_{\Lambda_b}^2 \ ,\end{aligned} \tag{B10}$$

$$\begin{aligned}\Omega^{(f)} = {} & \frac{1}{8z_1(1-z_1)z_2(1-z_2)} \frac{\sqrt{B_f}}{\sqrt{|Z_f|}} \left\{ K_1\left(\sqrt{Z_f B_f}\right)\ \theta(Z_f) \right. \\ & \left. + \frac{\pi}{2}\left[N_1\left(\sqrt{|Z_f| B_f}\right) - iJ_1\left(\sqrt{|Z_f| B_f}\right)\right]\ \theta(-Z_f) \right\} ,\end{aligned} \tag{B11}$$

with

$$\begin{aligned}B_f = {} & \frac{z_1(1-z_1)z_2(1-z_2)}{z_2 z_3} b_q^2 + \frac{z_2(1-z_2)}{z_3} [b_3' + (1-z_1) b_q]^2 \\ & + \left\{ b_2' - b_q z_1 - [b_3' + (1-z_1) b_q] z_2 \right\}^2 , \\ Z_f = {} & x_2 x_2' \rho M_{\Lambda_b}^2 (1-z_3) + \frac{z_3}{z_2(1-z_2)} \left\{ x_3 x_3' \rho M_{\Lambda_b}^2 (1-z_2) \right. \\ & + \frac{z_2}{z_1(1-z_1)} \left[\left(\frac{r^2}{4} - (1 - x_3 - y_1)(x_3'\rho + (1-y_1) r^2) \right) (1-z_1) \right. \\ & \left. \left. + \left(\frac{r^2}{4} + (x_2 - y_1)(x_2'\rho + y_1 r^2) \right) z_1 \right] M_{\Lambda_b}^2 \right\} ,\end{aligned} \tag{B12}$$

$$\begin{aligned}\Omega^{(g)} = {} & K_0\left(\sqrt{x_2 x_2' \rho} M_{\Lambda_b} b_2\right) K_0\left(\sqrt{x_3 x_3' \rho} M_{\Lambda_b}(b_3' + b_q)\right) \\ & \times K_0\left(\sqrt{x_3 + x_2'(1-x_3)\rho} M_{\Lambda_b} |b_2 - b_2'|\right) \left\{ K_0\left(\sqrt{Z_g} M_{\Lambda_b} b_q\right)\ \theta(Z_g) \right. \\ & \left. + \frac{\pi}{2}\left[-N_0\left(\sqrt{|Z_g|} M_{\Lambda_b} b_q\right) + iJ_0\left(\sqrt{|Z_g|} M_{\Lambda_b} b_q\right)\right]\ \theta(-Z_g) \right\} ,\end{aligned} \tag{B13}$$

with

$$Z_g = \frac{r^2}{4} - (1 - x_3 - y_1)[x_3'\rho + (1-y_1) r^2] \ , \tag{B14}$$

$$\begin{aligned}\Omega^{(h)} = {} & \frac{1}{4z_1(1-z_1)} \frac{\sqrt{B_h}}{\sqrt{|Z_h|}} K_0\left(\sqrt{x_3 x_3' \rho} M_{\Lambda_b} |b_3 - b_q|\right) \left\{ K_1\left(\sqrt{Z_h B_h}\right)\ \theta(Z_h) \right. \\ & \left. + \frac{\pi}{2}\left[N_1\left(\sqrt{|Z_h| B_h}\right) - iJ_1\left(\sqrt{|Z_h| B_h}\right)\right]\ \theta(-Z_h) \right\} ,\end{aligned} \tag{B15}$$

with

$$\begin{aligned}
B_h &= \frac{z_1(1-z_1)}{z_2} b_q^2 + (b_2' - z_1 b_q)^2 \ , \\
Z_h &= x_2 x_2' \rho M_{\Lambda_b}^2 (1-z_2) + \frac{z_2}{z_1(1-z_1)} \left\{ \left[\frac{r^2}{4} + (1-x_1-y_1)(1-x_1'\rho-(1-y_1)r^2) \right] z_1 \right. \\
&\quad \left. + \left[\frac{r^2}{4} + (x_3-y_1)(x_3'\rho + y_1 r^2) \right] (1-z_1) \right\} M_{\Lambda_b}^2 \ ,
\end{aligned} \tag{B16}$$

$$\begin{aligned}
\Omega^{(i)} &= K_0\left(\sqrt{x_2 x_2' \rho} M_{\Lambda_b} b_2\right) K_0\left(\sqrt{x_3 x_3' \rho} M_{\Lambda_b} |b_3' - b_q|\right) \\
&\quad \times K_0\left(\sqrt{x_3 + x_2'(1-x_3)\rho} M_{\Lambda_b} |b_2 - b_2'|\right) \left\{ K_0\left(\sqrt{Z_i} M_{\Lambda_b} b_q\right) \ \theta(Z_i) \right. \\
&\quad \left. + \frac{\pi}{2} \left[-N_0\left(\sqrt{|Z_i|} M_{\Lambda_b} b_q\right) + i J_0\left(\sqrt{|Z_i|} M_{\Lambda_b} b_q\right) \right] \ \theta(-Z_i) \right\} ,
\end{aligned} \tag{B17}$$

with

$$Z_i = \frac{r^2}{4} + (x_3 - y)(x_3'\rho + y r^2) \ , \tag{B18}$$

$$\Omega^{(j)} = \frac{1}{4 z_1(1-z_1)} \frac{\sqrt{B_j}}{\sqrt{Z_j}} K_0\left(\sqrt{x_2 x_2' \rho} M_{\Lambda_b} b_2\right) K_1\left(\sqrt{Z_j B_j}\right) \ , \tag{B19}$$

with

$$\begin{aligned}
B_j &= \frac{z_1(1-z_1)}{z_2} (b_2 - b_2')^2 + [b_3' - z_1(b_2 - b_2')]^2 \ , \\
Z_j &= \frac{z_2}{z_1(1-z_1)} \left\{ (1-x_1')(1-z_1)\rho + [x_3 + x_2'(1-x_3)\rho] z_1 \right\} M_{\Lambda_b}^2 \\
&\quad + x_3 x_3' \rho M_{\Lambda_b}^2 (1-z_2) \ ,
\end{aligned} \tag{B20}$$

$$\begin{aligned}
\Omega^{(k)} &= K_0\left(\sqrt{(1-x_1)(1-x_1')\rho} M_{\Lambda_b} b_2'\right) K_0\left(\sqrt{x_3 x_3' \rho} M_{\Lambda_b} |b_2 - b_3|\right) \\
&\quad \times K_0\left(\sqrt{(1-x_1) x_3' \rho} M_{\Lambda_b} |b_2 - b_2' - b_3 + b_3'|\right) K_0\left(\sqrt{(1-x_1)\rho} M_{\Lambda_b} |b_3 - b_3'|\right) \ ,
\end{aligned} \tag{B21}$$

$$\begin{aligned}
\Omega^{(l)} &= K_0\left(\sqrt{(1-x_1)(1-x_1')\rho} M_{\Lambda_b} |b_2 - b_3 + b_3'|\right) K_0\left(\sqrt{x_3 x_3' \rho} M_{\Lambda_b} |b_2' - b_3'|\right) \\
&\quad K_0\left(\sqrt{x_3(1-x_1')\rho} M_{\Lambda_b} |b_2 - b_2' - b_3 + b_3'|\right) K_0\left(\sqrt{(1-x_1)\rho} M_{\Lambda_b} |b_3 - b_3'|\right) \ ,
\end{aligned} \tag{B22}$$

$$\begin{aligned}
\Omega^{(m)} &= K_0\left(\sqrt{(1-x_1)(1-x_1')\rho} M_{\Lambda_b} (b_2' + b_q)\right) K_0\left(\sqrt{x_3 x_3' \rho} M_{\Lambda_b} |b_2 - b_3'|\right) \\
&\quad \times K_0\left(\sqrt{(1-x_1) x_3' \rho} M_{\Lambda_b} |b_2 - b_2'|\right) \left\{ K_0\left(\sqrt{Z_m} M_{\Lambda_b} b_q\right) \theta(Z_m) \right. \\
&\quad \left. + \frac{\pi}{2} \left[-N_0\left(\sqrt{|Z_m|} M_{\Lambda_b} b_q\right) + i\, J_0\left(\sqrt{|Z_m|} M_{\Lambda_b} b_q\right) \right] \theta(-Z_m) \right\} ,
\end{aligned} \tag{B23}$$

with

$$Z_m = \frac{r^2}{4} + (y_1 - x_1)[1 - y_1 r^2 - x_1' \rho] \;, \tag{B24}$$

$$\begin{aligned}\Omega^{(n)} = {} & K_0\left(\sqrt{(1-x_1)(1-x_1')\rho} M_{\Lambda_b}(b_2+b_q)\right) K_0\left(\sqrt{x_3 x_3' \rho} M_{\Lambda_b}|b_2'-b_3'|\right) \\ & \times K_0\left(\sqrt{x_3(1-x_1')\rho} M_{\Lambda_b}|b_2-b_2'|\right) \left\{ K_0\left(\sqrt{Z_n} M_{\Lambda_b} b_q\right) \theta(Z_n) \right. \\ & \left. + \frac{\pi}{2}\left[-N_0\left(\sqrt{|Z_n|} M_{\Lambda_b} b_q\right) + i\, J_0\left(\sqrt{|Z_n|} M_{\Lambda_b} b_q\right)\right] \theta(-Z_n) \right\} \;,\end{aligned} \tag{B25}$$

with

$$Z_n = \frac{r^2}{4} + (y_1 - x_1)[1 - y_1 r^2 - x_1' \rho] \;, \tag{B26}$$

$$\begin{aligned}\Omega^{(o)} = {} & K_0\left(\sqrt{(1-x_1)(1-x_1')\rho} M_{\Lambda_b}|b_2'-b_q|\right) K_0\left(\sqrt{x_3 x_3' \rho} M_{\Lambda_b}|b_2-b_3'|\right) \\ & \times K_0\left(\sqrt{(1-x_1)x_3'\rho} M_{\Lambda_b}|b_2-b_2'|\right) \left\{ K_0\left(\sqrt{Z_o} M_{\Lambda_b} b_q\right) \theta(Z_o) \right. \\ & \left. + \frac{\pi}{2}\left[-N_0\left(\sqrt{|Z_o|} M_{\Lambda_b} b_q\right) + i\, J_0\left(\sqrt{|Z_o|} M_{\Lambda_b} b_q\right)\right] \theta(-Z_o) \right\} \;,\end{aligned} \tag{B27}$$

with

$$Z_o = \frac{r^2}{4} + (1 - x_1 - y_1)[1 - (1-y_1) r^2 - x_1' \rho] \;, \tag{B28}$$

$$\begin{aligned}\Omega^{(p)} = {} & K_0\left(\sqrt{(1-x_1)(1-x_1')\rho} M_{\Lambda_b}|b_2-b_q|\right) K_0\left(\sqrt{x_3 x_3' \rho} M_{\Lambda_b}|b_2'-b_3'|\right) \\ & K_0\left(\sqrt{x_3(1-x_1')\rho} M_{\Lambda_b}|b_2-b_2'|\right) \left\{ K_0\left(\sqrt{Z_p} M_{\Lambda_b} b_q\right) \theta(Z_p) \right. \\ & \left. + \frac{\pi}{2}\left[-N_0\left(\sqrt{|Z_p|} M_{\Lambda_b} b_q\right) + i\, J_0\left(\sqrt{|Z_p|} M_{\Lambda_b} b_q\right)\right] \theta(-Z_p) \right\} \;,\end{aligned} \tag{B29}$$

with

$$Z_p = \frac{r^2}{4} + (1 - x_1 - y_1)[1 - (1-y_1) r^2 - x_1' \rho] \;, \tag{B30}$$

$$\begin{aligned}\Omega^{(q)} = {} & K_0\left(\sqrt{(1-x_1)(1-x_1')\rho} M_{\Lambda_b}|b_2'+b_3-b_3'|\right) K_0\left(\sqrt{x_3 x_3' \rho} M_{\Lambda_b}|b_2-b_3|\right) \\ & \times K_0\left(\sqrt{(1-x_1)x_3'\rho} M_{\Lambda_b}|b_2-b_2'-b_3+b_3'|\right) K_0\left(\sqrt{(1-x_1)\rho} M_{\Lambda_b}|b_3-b_3'|\right) \;,\end{aligned} \tag{B31}$$

$$\begin{aligned}\Omega^{(r)} = {} & K_0\left(\sqrt{(1-x_1)(1-x_1')\rho} M_{\Lambda_b} b_2\right) K_0\left(\sqrt{x_3 x_3' \rho} M_{\Lambda_b}|b_2'-b_3'|\right) \\ & \times K_0\left(\sqrt{x_3(1-x_1')\rho} M_{\Lambda_b}|b_2-b_2'-b_3+b_3'|\right) K_0\left(\sqrt{(1-x_1)\rho} M_{\Lambda_b}|b_3-b_3'|\right) \;.\end{aligned} \tag{B32}$$

APPENDIX C: EXPRESSIONS OF H_F^{IJ}

The part H_F^{ij} of the hard amplitudes, that varies among the spin structures of the three valence quarks in the Λ baryon and among the form factors $A_{1,2}$ and $B_{1,2}$, are gathered in the following tables. Their derivation is similar to that presented in [33] for the proton form factor. The contributions to H_F^{ij} from Figs. 1(a), 1(k), 1(l), 1(n), 1(p), and 1(r) vanish.

F	j	$H_F^{(b)j}$
A_1	V	$-8r(1-r^2)^2M_{\Lambda_b}^5(1-x_2')$
	A	$8r(1-r^2)^2M_{\Lambda_b}^5(1-x_2')$
	T	$24r(1-r^2)^2M_{\Lambda_b}^5(1-x_2')$
A_2	V	$16r(1-r^2)M_{\Lambda_b}^5(1-x_2')(1-2y)$
	A	$-16r(1-r^2)M_{\Lambda_b}^5(1-x_2')(1-2y)$
	T	$-48r(1-r^2)M_{\Lambda_b}^5(1-x_2')(1-2y)$
B_1	V	$8r(1-r^2)^2M_{\Lambda_b}^5(1-x_2')$
	A	$-8r(1-r^2)^2M_{\Lambda_b}^5(1-x_2')$
	T	$-24r(1-r^2)^2M_{\Lambda_b}^5(1-x_2')$
B_2	V	$16r(1-r^2)M_{\Lambda_b}^5(1-x_2')(1-2y)$
	A	$-16r(1-r^2)M_{\Lambda_b}^5(1-x_2')(1-2y)$
	T	$-48r(1-r^2)M_{\Lambda_b}^5(1-x_2')(1-2y)$

F	j	$H_F^{(c)j}$
A_1	V	$16r(1-r^2)^2M_{\Lambda_b}^5(1-x_2')y$
	A	$-16r(1-r^2)^2M_{\Lambda_b}^5(1-x_2')y$
	T	$-48r(1-r^2)^2M_{\Lambda_b}^5(1-x_2')y$
A_2	V	0
	A	0
	T	0
B_1	V	$-16r(1-r^2)^2M_{\Lambda_b}^5(1-x_2')y$
	A	$16r(1-r^2)^2M_{\Lambda_b}^5(1-x_2')y$
	T	$48r(1-r^2)^2M_{\Lambda_b}^5(1-x_2')y$
B_2	V	0
	A	0
	T	0

F	j	$H_F^{(d)j}$
A_1	V	$16r(1-r^2)^2M_{\Lambda_b}^5(1-x_2')$
	A	$-16r(1-r^2)^2M_{\Lambda_b}^5(1-x_2')$
	T	$-48r(1-r^2)^2M_{\Lambda_b}^5(1-x_2')$
A_2	V	0
	A	0
	T	0
B_1	V	$-16r(1-r^2)^2M_{\Lambda_b}^5(1-x_2')$
	A	$16r(1-r^2)^2M_{\Lambda_b}^5(1-x_2')$
	T	$48r(1-r^2)^2M_{\Lambda_b}^5(1-x_2')$
B_2	V	0
	A	0
	T	0

F	j	$H_F^{(e)j}$
A_1	V	$4r(1-r^2)M_{\Lambda_b}^5(6+r^2-2x_1'+2r^2x_1'+2x_3'-2r^2x_3' - 12y-4r^2y+4x_1'y-4r^2x_1'y+4y^2+4r^2y^2)$
	A	$-4r(1-r^2)M_{\Lambda_b}^5(6+r^2-2x_1'+2r^2x_1'+2x_3'-2r^2x_3' - 12y-4r^2y+4x_1'y-4r^2x_1'y+4y^2+4r^2y^2)$
	T	$-8r(1-r^2)M_{\Lambda_b}^5(5+r^2-x_1'+r^2x_1'+x_3'-r^2x_3'-10y - 2r^2y+2x_1'y-2r^2x_1'y+4y^2+2r^2y^2)$
A_2	V	$16r(1-r^2)M_{\Lambda_b}^5(1+x_1'+x_3'-4y+2y^2)$
	A	$-16r(1-r^2)M_{\Lambda_b}^5(1+x_1'+x_3'-4y+2r^2)$
	T	$-16r(1-r^2)M_{\Lambda_b}^5(3+x_1'+x_3'-8y+4y^2)$
B_1	V	$-4r(1-r^2)M_{\Lambda_b}^5(-2+r^2-2x_1'+2r^2x_1'+2x_3'-2r^2x_3' - 4r^2y+4y+4x_1'y-4r^2x_1'y-4y^2+4r^2y^2)$
	A	$4r(1-r^2)M_{\Lambda_b}^5(-2+r^2-2x_1'+2r^2x_1'+2x_3'-2r^2x_3' - 4r^2y+4y+4x_1'y-4r^2x_1'y-4y^2+4r^2y^2)$
	T	$-8r(1-r^2)M_{\Lambda_b}^5(3-r^2+x_1'-r^2x_1'-x_3'+r^2x_3'-6y + 2r^2y-2x_1'y+2r^2x_1'y+4y^2-2r^2y^2)$
B_2	V	$16rM_{\Lambda_b}^5(1-3x_1'+3r^2x_1'+x_3'-r^2x_3'-2r^2y+4x_1'y - 4r^2x_1'y-2y^2+2r^2y^2)$
	A	$-16rM_{\Lambda_b}^5(1-3x_1'+3r^2x_1'+x_3'-r^2x_3'-2r^2y+4x_1'y - 4r^2x_1'y-2y^2+2r^2y^2)$
	T	$16rM_{\Lambda_b}^5(1+r^2+3x_1'-3r^2x_1'-x_3'+r^2x_3'-2r^2y-4y - 4x_1'y+4r^2x_1'y+4y^2)$

F	j	$H_F^{(f)j}$
A_1	V	$-16r(1-r^2)M_{\Lambda_b}^5(1-y)^2$
	A	$16r(1-r^2)M_{\Lambda_b}^5(1-y)^2$
	T	$8r(1-r^2)M_{\Lambda_b}^5(3-5y+2r^2y+2x_3'y-2r^2x_3'y+2y^2-2r^2y^2)$
A_2	V	$-32r(1-r^2)M_{\Lambda_b}^5(1-y)^2$
	A	$32r(1-r^2)M_{\Lambda_b}^5(1-y)^2$
	T	$16r(1-r^2)M_{\Lambda_b}^5(3-2y)(1-y)$
B_1	V	$-16r(1-r^2)M_{\Lambda_b}^5(1-y)^2$
	A	$16r(1-r^2)M_{\Lambda_b}^5(1-y)^2$
	T	$-8r(1-r^2)M_{\Lambda_b}^5(-3+5y+2r^2y+2x_3'y-2r^2x_3'y-2y^2-2r^2y^2)$
B_2	V	$32rM_{\Lambda_b}^5(1-y)(1-y-r^2y)$
	A	$32rM_{\Lambda_b}^5(1-y)(-1+y+r^2y)$
	T	$16rM_{\Lambda_b}^5(-3+5y+5r^2y+4x_3'y-4r^2x_3'y-2y^2-6r^2y^2)$

F	j	$H_F^{(g)j}$
A_1	V	$-8r(1-r^2)M_{\Lambda_b}^5(2+x_2'-r^2x_2'-2y-2x_2'y+2r^2x_2'y)$
	A	$8r(1-r^2)M_{\Lambda_b}^5(2+x_2'-r^2x_2'-2y-2x_2'y+2r^2x_2'y)$
	T	$8r(1-r^2)M_{\Lambda_b}^5(4+2r^2+x_2'-r^2x_2'+2x_3'-2r^2x_3'-4y-2r^2y-2x_2'y+2r^2x_2'y)$
A_2	V	$16r(1-r^2)M_{\Lambda_b}^5(-2+2y+x_2')$
	A	$-16r(1-r^2)M_{\Lambda_b}^5(-2+2y+x_2')$
	T	$16r(1-r^2)M_{\Lambda_b}^5(4-x_2'-4y)$
B_1	V	$-8r(1-r^2)M_{\Lambda_b}^5(2-x_2'+r^2x_2'-2y+2x_2'y-2r^2x_2'y)$
	A	$8r(1-r^2)M_{\Lambda_b}^5(2-x_2'+r^2x_2'-2y+2x_2'y-2r^2x_2'y)$
	T	$-8r(1-r^2)M_{\Lambda_b}^5(-4+2r^2+x_2'-r^2x_2'+2x_3'-2r^2x_3'+4y-2r^2y-2x_2'y+2r^2x_2'y)$
B_2	V	$16rM_{\Lambda_b}^5(2-3x_2'+3r^2x_2'-2y-2r^2y+4x_2'y-4r^2x_2'y)$
	A	$-16rM_{\Lambda_b}^5(2-3x_2'+3r^2x_2'-2y-2r^2y+4x_2'y-4r^2x_2'y)$
	T	$16rM_{\Lambda_b}^5(-4+2r^2+3x_2'-3r^2x_2'+4x_3'-4r^2x_3'+8y-4r^2y-4x_2'y+4r^2x_2'y)$

F	j	$H_F^{(h)j}$
A_1	V	$-8r(1-r^2)M_{\Lambda_b}^5(r^2-y-r^2y-2x_3'y+2r^2x_3'y-2r^2y^2)$
	A	$8r(1-r^2)M_{\Lambda_b}^5(r^2-y-r^2y-2x_3'y+2r^2x_3'y-2r^2y^2)$
	T	$4r(1-r^2)M_{\Lambda_b}^5(3r^2-6y-6r^2y-4x_3'y+4r^2x_3'y+4y^2-4r^2y^2)$
A_2	V	$16r(1-r^2)M_{\Lambda_b}^5y$
	A	$-16r(1-r^2)M_{\Lambda_b}^5y$
	T	$16r(1-r^2)M_{\Lambda_b}^5y(-3+2y)$
B_1	V	$8r(1-r^2)M_{\Lambda_b}^5(r^2+y-r^2y-2x_3'y+2r^2x_3'y-2r^2y^2)$
	A	$-8r(1-r^2)M_{\Lambda_b}^5(r^2+y-r^2y-2x_3'y+2r^2x_3'y-2r^2y^2)$
	T	$-4r(1-r^2)M_{\Lambda_b}^5(3r^2+6y-6r^2y-4x_3'y+4r^2x_3'y-4y^2-4r^2y^2)$
B_2	V	$-16r(1-r^2)M_{\Lambda_b}^5y$
	A	$16r(1-r^2)M_{\Lambda_b}^5y$
	T	$-16r(1-r^2)M_{\Lambda_b}^5y(-3+2y)$

F	j	$H_F^{(i)j}$
A_1	V	$8r(1-r^2)M_{\Lambda_b}^5(1+r^2-2x_3'+2r^2x_3'-2r^2y)$
	A	$-8r(1-r^2)M_{\Lambda_b}^5(1+r^2-2x_3'+2r^2x_3'-2r^2y)$
	T	$-8r(1-r^2)M_{\Lambda_b}^5(3+3r^2-4x_3'+4r^2x_3'-2y-4r^2y)$
A_2	V	$16r(1-r^2)M_{\Lambda_b}^5(1-2x_2'y)$
	A	$-16r(1-r^2)M_{\Lambda_b}^5(1-2x_2'y)$
	T	$16r(1-r^2)M_{\Lambda_b}^5(-3+2y+2x_2'y)$
B_1	V	$8r(1-r^2)M_{\Lambda_b}^5(1-r^2+2x_3'-2r^2x_3'+2r^2y)$
	A	$-8r(1-r^2)M_{\Lambda_b}^5(1-r^2+2x_3'-2r^2x_3'+2r^2y)$
	T	$-8r(1-r^2)M_{\Lambda_b}^5(3-3r^2+4x_3'-4r^2x_3'-2y+4r^2y)$
B_2	V	$-16r(1-r^2)M_{\Lambda_b}^5(1-2x_2'y)$
	A	$16r(1-r^2)M_{\Lambda_b}^5(1-2x_2'y)$
	T	$16r(1-r^2)M_{\Lambda_b}^5(3-2y-2x_2'y)$

F	j	$H_F^{(j)j}$
A_1	V	$16r(1-r^2)M_{\Lambda_b}^5(1-x_2'+r^2x_2')$
	A	$-16r(1-r^2)M_{\Lambda_b}^5(1-x_2'+r^2x_2')$
	T	$-16r(1-r^2)M_{\Lambda_b}^5(3-x_2'+r^2x_2')$
A_2	V	$32r(1-r^2)M_{\Lambda_b}^5(1-x_2')$
	A	$-32r(1-r^2)M_{\Lambda_b}^5(1-x_2')$
	T	$32r(1-r^2)M_{\Lambda_b}^5(-2+x_2')$
B_1	V	$16r(1-r^2)M_{\Lambda_b}^5(1+x_2'-r^2x_2')$
	A	$-16r(1-r^2)M_{\Lambda_b}^5(1+x_2'-r^2x_2')$
	T	$-16r(1-r^2)M_{\Lambda_b}^5(1+x_2'-r^2x_2')$
B_2	V	$-32r(1-r^2)M_{\Lambda_b}^5(1+x_2')$
	A	$32r(1-r^2)M_{\Lambda_b}^5(1+x_2')$
	T	$32r(1-r^2)M_{\Lambda_b}^5(2x_1'+x_2')$

F	j	$H_F^{(m)j}$
A_1	V	$-8r(1-r^2)^2 M_{\Lambda_b}^5 x_3'$
	A	$8r(1-r^2)^2 M_{\Lambda_b}^5 x_3'$
	T	$-8r(1-r^2)^2 M_{\Lambda_b}^5 x_3'$
A_2	V	$16r(1-r^2) M_{\Lambda_b}^5 (1-2y) x_3'$
	A	$-16r(1-r^2) M_{\Lambda_b}^5 (1-2y) x_3'$
	T	$16r(1-r^2) M_{\Lambda_b}^5 (1-2y) x_3'$
B_1	V	$8r(1-r^2)^2 M_{\Lambda_b}^5 x_3'$
	A	$-8r(1-r^2)^2 M_{\Lambda_b}^5 x_3'$
	T	$8r(1-r^2)^2 M_{\Lambda_b}^5 x_3'$
B_2	V	$16r(1-r^2) M_{\Lambda_b}^5 (1-2y) x_3'$
	A	$-16r(1-r^2) M_{\Lambda_b}^5 (1-2y) x_3'$
	T	$16r(1-r^2) M_{\Lambda_b}^5 (1-2y) x_3'$

F	j	$H_F^{(o)j}$
A_1	V	$16r(1-r^2)^2 M_{\Lambda_b}^5 y x_3'$
	A	$-16r(1-r^2)^2 M_{\Lambda_b}^5 y x_3'$
	T	$16r(1-r^2)^2 M_{\Lambda_b}^5 y x_3'$
A_2	V	0
	A	0
	T	0
B_1	V	$-16r(1-r^2)^2 M_{\Lambda_b}^5 y x_3'$
	A	$16r(1-r^2)^2 M_{\Lambda_b}^5 y x_3'$
	T	$-16r(1-r^2)^2 M_{\Lambda_b}^5 y x_3'$
B_2	V	0
	A	0
	T	0

F	j	$H_F^{(q)j}$
A_1	V	$16r(1-r^2)^2 M_{\Lambda_b}^5 x_3'$
	A	$-16r(1-r^2)^2 M_{\Lambda_b}^5 x_3'$
	T	$16r(1-r^2)^2 M_{\Lambda_b}^5 x_3'$
A_2	V	0
	A	0
	T	0
B_1	V	$-16r(1-r^2)^2 M_{\Lambda_b}^5 x_3'$
	A	$16r(1-r^2)^2 M_{\Lambda_b}^5 x_3'$
	T	$-16r(1-r^2)^2 M_{\Lambda_b}^5 x_3'$
B_2	V	0
	A	0
	T	0

---

[1] H.H. Shih, S.C. Lee, and H-n. Li, Phys. Rev. D **59**, 094014 (1999).

[2] H.H. Shih, S.C. Lee, and H-n. Li, Phys. Rev. D **61**, 114002 (2000).

[3] H.H. Shih, S.C. Lee, and H-n. Li, Chin. J. Phys. **39**, 328 (2001).

[4] H-n. Li and H.L. Yu, Phys. Rev. Lett. **74**, 4388 (1995); Phys. Lett. B **353**, 301 (1995); Phys. Rev. D **53**, 2480 (1996); H-n. Li, Phys. Lett. B **348**, 597 (1995).

[5] H-n. Li, Phys. Rev. D **52**, 3958 (1995).

[6] C. H. Chang and H-n. Li, Phys. Rev. D **55**, 5577 (1997).

[7] T.W. Yeh and H-n. Li, Phys. Rev. D **56**, 1615 (1997); H-n. Li and B. Melic, Eur. Phys. J. C **11**, 695 (1999).

[8] C.Y. Wu, T.W. Yeh, and H-n. Li, Phys. Rev. D **53**, 4982 (1996); Phys. Rev. D **55**, 237 (1997).
[9] M. Bauer, B. Stech, and M. Wirbel, Z. Phys. C **29**, 637 (1985); Z. Phys. C **34**, 103 (1987).
[10] H-n. Li, hep-ph/0103305; hep-ph/0110365.
[11] G.R. Farrar, H. Zhang, A.A. Ogloblin, and I.R. Zhitnitsky, Nucl. Phys. **B311**, 585 (1989).
[12] V.L. Chernyak, A.A. Ogloblin, and I.R. Zhitnitsky, Z. Phys. C **42**, 569 (1989).
[13] H.Y. Cheng and B. Tseng, Phys. Rev. D **53**, 1457 (1997); D **55**, 1697(E) (1997).
[14] H.Y. Cheng, H-n. Li, and K.C. Yang, Phys. Rev. D **60**, 094005 (1999).
[15] J.C. Collins and D.E. Soper, Nucl. Phys. **B193**, 381 (1981).
[16] J. Botts and G. Sterman, Nucl. Phys. **B325**, 62 (1989).
[17] H-n. Li and G. Sterman, Nucl. Phys. **B381**, 129 (1992).
[18] T. Kurimoto, H-n. Li, and A.I. Sanda, Phys. Rev. D **65**, 014007 (2002).
[19] A. Ali and C. Greub, Phys. Rev. D **57**, 2996 (1998).
[20] H.Y. Cheng and B. Tseng, Phys. Rev. D **58**, 094005 (1998).
[21] M. Beneke, G. Buchalla, M. Neubert, and C.T. Sachrajda, Phys. Rev. Lett. **83**, 1914 (1999); Nucl. Phys. **B591**, 313 (2000).
[22] C.H. Chen, Y.Y. Keum, and H-n. Li, Phys. Rev. D **64**, 112002 (2001).
[23] W. Loinaz and R. Akhoury, Phys. Rev. D **53**, 1416 (1996).
[24] Y.Y. Keum, H-n. Li and A.I. Sanda, Phys. Lett. B **504**, 6 (2001); Phys. Rev. D **63**, 054008 (2001).
[25] F. Schlumpf, Ph. D. thesis, 1992, hep-ph/9211255;
[26] C.E. Carlson and J. Milana, Phys. Rev. D **49**, 5908 (1994).
[27] Particle Data Group, C. Caso *et al.*, Euro. Phys. J. C **3**, 1 (1998).
[28] Fayyazuddin and Riazuddin, Phys. Rev. D **58**, 014016 (1998).
[29] R. Mohanta *et al.*, Prog. Theor. Phys. **101**, 959 (1999).
[30] H-n. Li, talk presented at the 5th KEK Topical Conference–Frontiers in Flavor Physics, Tokyo, Japan, Nov. 19-22, 2001.
[31] Belle Coll., K. Abe *et al.*, hep-ex/0109021.
[32] CLEO Coll., T.E. Coan, hep-ex/0110055.
[33] H-n. Li, Phys. Rev. D **48**, 4243 (1993); B. Kundu, H-n. Li, J. Samuelsson, and P. Jain, Eur. Phys. J. C **8**, 637 (1999).

Table I: The hard scales t_1^i and t_2^i for each diagram i in Fig. 1.

i	t_1^i	t_2^i
(a)	$\max(\sqrt{x_2x_2'\rho}M_{\Lambda_b}, \frac{1}{\lvert b_2\rvert})$	$\max(\sqrt{x_3x_3'\rho}M_{\Lambda_b}, \frac{1}{\lvert b_3'\rvert})$
(b)	$\max(\sqrt{x_2x_2'\rho}M_{\Lambda_b}, \frac{1}{\lvert b_2+b_q\rvert})$	$\max(\sqrt{x_3x_3'\rho}M_{\Lambda_b}, \frac{1}{\lvert b_3'\rvert})$
(c)	$\max(\sqrt{x_2x_2'\rho}M_{\Lambda_b}, \frac{1}{\lvert b_2-b_q\rvert})$	$\max(\sqrt{x_3x_3'\rho}M_{\Lambda_b}, \frac{1}{\lvert b_3'\rvert})$
(d)	$\max(\sqrt{x_2x_2'\rho}M_{\Lambda_b}, \frac{1}{\lvert b_2\rvert})$	$\max(\sqrt{x_3x_3'\rho}M_{\Lambda_b}, \frac{1}{\lvert b_3'\rvert})$
(e)	$\max(\sqrt{x_2x_2'\rho}M_{\Lambda_b}, \frac{1}{\lvert b_2\rvert})$	$\max(\sqrt{x_3x_3'\rho}M_{\Lambda_b}, \frac{1}{\lvert b_3'+b_q\rvert})$
(f)	$\max(\sqrt{x_2x_2'\rho}M_{\Lambda_b}, \frac{1}{\lvert b_2\rvert})$	$\max(\sqrt{x_3x_3'\rho}M_{\Lambda_b}, \frac{1}{\lvert b_3'+b_q\rvert})$
(g)	$\max(\sqrt{x_2x_2'\rho}M_{\Lambda_b}, \frac{1}{\lvert b_2\rvert})$	$\max(\sqrt{x_3x_3'\rho}M_{\Lambda_b}, \frac{1}{\lvert b_3'+b_q\rvert})$
(h)	$\max(\sqrt{x_2x_2'\rho}M_{\Lambda_b}, \frac{1}{\lvert b_2\rvert})$	$\max(\sqrt{x_3x_3'\rho}M_{\Lambda_b}, \frac{1}{\lvert b_3'-b_q\rvert})$
(i)	$\max(\sqrt{x_2x_2'\rho}M_{\Lambda_b}, \frac{1}{\lvert b_2\rvert})$	$\max(\sqrt{x_3x_3'\rho}M_{\Lambda_b}, \frac{1}{\lvert b_3'-b_q\rvert})$
(j)	$\max(\sqrt{x_2x_2'\rho}M_{\Lambda_b}, \frac{1}{\lvert b_2\rvert})$	$\max(\sqrt{x_3x_3'\rho}M_{\Lambda_b}, \frac{1}{\lvert b_3'\rvert})$
(k)	$\max(\sqrt{(1-x_1)(1-x_1')\rho}M_{\Lambda_b}, \frac{1}{\lvert b_2\rvert})$	$\max(\sqrt{x_3x_3'\rho}M_{\Lambda_b}, \frac{1}{\lvert b_1\rvert})$
(l)	$\max(\sqrt{(1-x_1)(1-x_1')\rho}M_{\Lambda_b}, \frac{1}{\lvert b_2-b_3+b_3'\rvert})$	$\max(\sqrt{x_3x_3'\rho}M_{\Lambda_b}, \frac{1}{\lvert b_1'\rvert})$
(m)	$\max(\sqrt{(1-x_1)(1-x_1')\rho}M_{\Lambda_b}, \frac{1}{\lvert b_2'+b_q\rvert})$	$\max(\sqrt{x_3x_3'\rho}M_{\Lambda_b}, \frac{1}{\lvert b_2-b_3'\rvert})$
(n)	$\max(\sqrt{(1-x_1)(1-x_1')\rho}M_{\Lambda_b}, \frac{1}{\lvert b_2+b_q\rvert})$	$\max(\sqrt{x_3x_3'\rho}M_{\Lambda_b}, \frac{1}{\lvert b_1'\rvert})$
(o)	$\max(\sqrt{(1-x_1)(1-x_1')\rho}M_{\Lambda_b}, \frac{1}{\lvert b_2'-b_q\rvert})$	$\max(\sqrt{x_3x_3'\rho}M_{\Lambda_b}, \frac{1}{\lvert b_2-b_3'\rvert})$
(p)	$\max(\sqrt{(1-x_1)(1-x_1')\rho}M_{\Lambda_b}, \frac{1}{\lvert b_2-b_q\rvert})$	$\max(\sqrt{x_3x_3'\rho}M_{\Lambda_b}, \frac{1}{\lvert b_1'\rvert})$
(q)	$\max(\sqrt{(1-x_1)(1-x_1')\rho}M_{\Lambda_b}, \frac{1}{\lvert b_2'-b_3'+b_3\rvert})$	$\max(\sqrt{x_3x_3'\rho}M_{\Lambda_b}, \frac{1}{\lvert b_2'-b_3'\rvert})$
(r)	$\max(\sqrt{(1-x_1)(1-x_1')\rho}M_{\Lambda_b}, \frac{1}{\lvert b_2\rvert})$	$\max(\sqrt{x_3x_3'\rho}M_{\Lambda_b}, \frac{1}{\lvert b_1'\rvert})$

Table II: The coefficients A_1, A_2, B_1, and B_2 from the transverse component ϕ^T of the Λ baryon distribution amplitudes for the choices of the hard scales,
(a) $t^i = \max\left(t_1^i, t_2^i, w, w', w_q\right)$, (b) $t^i = \max\left(\frac{t_1^i+t_2^i}{2}, w, w', w_q\right)$.

	(a)	(b)
A_1^T	$-7.17 \times 10^{-10} - 8.69 \times 10^{-9} i$	$-1.18 \times 10^{-9} - 1.54 \times 10^{-8} i$
A_2^T	$-5.91 \times 10^{-10} - 1.62 \times 10^{-8} i$	$5.97 \times 10^{-10} - 2.83 \times 10^{-8} i$
B_1^T	$6.54 \times 10^{-10} - 7.53 \times 10^{-9} i$	$1.14 \times 10^{-9} - 1.27 \times 10^{-8} i$
B_2^T	$2.63 \times 10^{-11} + 1.21 \times 10^{-8} i$	$6.36 \times 10^{-10} + 1.83 \times 10^{-8} i$

Table III: The $\Lambda_b \to \Lambda J/\psi$ branching ratios and the asymmetry parameters α derived in different approaches. The data are also shown.

	Ref. [13]	Ref. [28]	Ref. [29]	This work	Experimental data
$B(\Lambda_b \to \Lambda J/\psi)$	2.1×10^{-4}	6.04×10^{-4}	2.49×10^{-4}	$(1.65 \sim 5.27) \times 10^{-4}$	$(4.7 \pm 2.8) \times 10^{-4}$
α	-0.11	-0.18	-0.208	$-0.17 \sim -0.14$	-

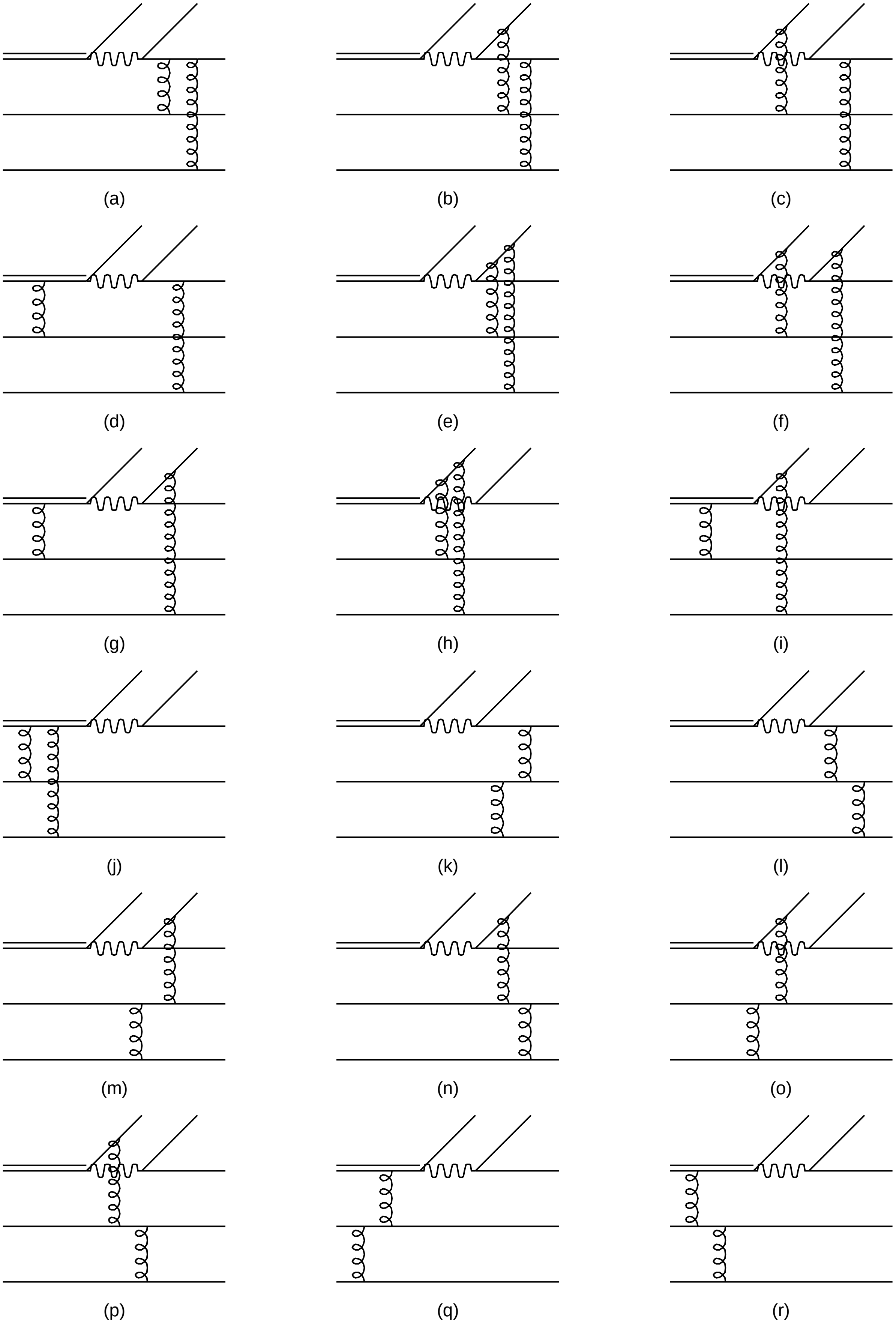

FIG. 1